



INSTITUT DE FRANCE  
Académie des sciences

# *Comptes Rendus*

---

## *Géoscience*

### *Sciences de la Planète*

Frederic Moynier, David A. Fike, Gabrielle Menard, Woodward W. Fischer, John P. Grotzinger and Arnaud Agranier

#### **Iron isotopes and the redox evolution of Ediacaran sediments**

Volume 352, issue 8 (2020), p. 579-588

Published online: 27 January 2021

<https://doi.org/10.5802/crgeos.44>



This article is licensed under the  
CREATIVE COMMONS ATTRIBUTION 4.0 INTERNATIONAL LICENSE.  
<http://creativecommons.org/licenses/by/4.0/>



*Les Comptes Rendus. Géoscience — Sciences de la Planète sont membres du  
Centre Mersenne pour l'édition scientifique ouverte*

[www.centre-mersenne.org](http://www.centre-mersenne.org)

e-ISSN : 1778-7025



Original Article — Petrology, Geochemistry

# Iron isotopes and the redox evolution of Ediacaran sediments

Frederic Moynier<sup>\*, a</sup>, David A. Fike<sup>b</sup>, Gabrielle Menard<sup>c</sup>, Woodward W. Fischer<sup>d</sup>,  
John P. Grotzinger<sup>d</sup> and Arnaud Agranier<sup>c</sup>

<sup>a</sup> Université de Paris, Institut de Physique du Globe de Paris, 1 rue Jussieu, 75238 Paris cedex 05, France

*F. Moynier a été lauréat d'un prix 2020 de l'Académie des sciences*

<sup>b</sup> Department of Earth and Planetary Sciences and McDonnell Center for the Space Sciences, Washington University, St. Louis, MO 63130, USA

<sup>c</sup> Institut Universitaire Européen de la Mer, Université de Brest, Place Nicolas Copernic, 29820 Plouzané, France

<sup>d</sup> Division of Geological and Planetary Sciences, California Institute of Technology, Pasadena, CA 91125, USA

*E-mails:* moynier@ipgp.fr (F. Moynier), dfike@levee.wustl.edu (D. A. Fike), G.menard@opgc.univ-bpclermont.fr (G. Menard), wfischer@caltech.edu (W. W. Fischer), grotz@gps.caltech.edu (J. P. Grotzinger), arnaud.agranier@univ-brest.fr (A. Agranier)

**Abstract.** The Ediacaran age (ca. 570 Ma) Shuram excursion, a ca. 12‰ depletion in  $\delta^{13}\text{C}_{\text{carb}}$ , may record a dramatic oxidation of marine sediments associated with a reorganization of Earth's carbon cycle closely preceding the rise of large metazoans. However, several geochemical indicators suggest it may instead record secondary processes affecting the sediments such as post-depositional alteration. The stable isotopic composition of iron incorporated within carbonates ( $\delta^{56}\text{Fe}_{\text{carb}}$ ) reveals an anomalous  $^{56}\text{Fe}$ -depletion (down to  $-1.05\%$ ) in strata containing the Shuram excursion, while the underlying and overlying strata have crustal  $\delta^{56}\text{Fe}_{\text{carb}}$  values. These depleted  $\delta^{56}\text{Fe}_{\text{carb}}$  data during the Shuram excursion reflect incomplete reduction of iron oxides, limited by low ambient organic carbon contents. This elevated pulse of sedimentary iron oxides would consume the majority of the limited pool of organic carbon and therefore would give rise to very low net organic carbon burial during a time of enhanced detrital delivery of oxidized iron to the sediments. These results imply a syndepositional origin for the Shuram excursion, which represents a shift in the redox composition of Earth's sedimentary shell toward more oxidizing conditions, perhaps removing a long-lived buffer on atmospheric oxygen.

**Keywords.** Geochemistry, Ediacara, Shuram excursion, Fe isotopes, Oxygenation, Redox change, Ocean.

*Manuscript received 18th September 2020, revised 15th December 2020, accepted 18th December 2020.*

\* Corresponding author.

## 1. Introduction

Metazoa first appeared in the fossil record during the Ediacaran Period. A variety of paleoenvironmental proxy records suggest a possible association of metazoan evolution with a perturbation in the redox structure of the atmosphere and ocean basins [Canfield *et al.*, 2007, Fike *et al.*, 2006, McFadden *et al.*, 2008]. Specifically, the Shuram excursion, the largest negative carbonate carbon isotope excursion ( $\delta^{13}\text{C}_{\text{carb}}$ ) in the sedimentary record, is observed globally in strata of this age [e.g., Burns and Matter, 1993, Grotzinger *et al.*, 2011, Le Guerroue *et al.*, 2006a]. The Shuram excursion has been suggested to represent a major perturbation in the marine carbon cycle and concomitant perturbation to the redox structure of the fluid Earth [e.g., Fike *et al.*, 2006].

However, several aspects of the Shuram excursion (most notably, frequent covariation of  $\delta^{13}\text{C}_{\text{carb}}$  and  $\delta^{18}\text{O}_{\text{carb}}$  isotope ratios and the lack of a similar excursion in organic carbon isotopes ( $\delta^{13}\text{C}_{\text{org}}$ ) in strata with low total organic carbon (TOC) abundance), have resulted in suggestions that this stratigraphic pattern instead resulted from post-depositional processes, ranging from interaction with meteoric fluids [Knauth and Kennedy, 2009, Swart, 2008] to late-stage burial diagenesis [Derry, 2010a,b]. Each of these alteration hypotheses fails to explain the widespread occurrence of the Shuram excursion (and its correlatives) during mid-Ediacaran time, as these diagenetic processes are intrinsically local—and not temporally restricted to mid-Ediacaran age strata. A third mechanism—global diagenesis [Grotzinger *et al.*, 2011]—combines aspects of each of these hypotheses. It differs, however, in that this hypothesis is fundamentally driven by a global and synchronous change in the redox composition of the sediments (toward a more oxidizing bulk composition) at the time of deposition, resulting in a sedimentary reactor that was preconditioned to produce a widespread  $\delta^{13}\text{C}_{\text{carb}}$  excursion of similar magnitude in basins around the world [Calver, 2000, Fike *et al.*, 2006, Kaufman *et al.*, 2007, McFadden *et al.*, 2008].

In recent years, there is increasing evidence that the  $\delta^{13}\text{C}$  signature of the Shuram was acquired at the time of deposition. While, the general lack of covariation between  $\delta^{13}\text{C}_{\text{carb}}$  and bulk  $\delta^{13}\text{C}_{\text{org}}$  is also seen in coeval high TOC sections [Lee *et al.*, 2013], certain lipid biomarker classes record a smaller magnitude

excursion in parallel with that observed in  $\delta^{13}\text{C}_{\text{carb}}$ , supporting a primary origin for the Shuram excursion [Lee *et al.*, 2015]. Further, detailed stratigraphic analysis from the equivalent sections in Australia [Husson *et al.*, 2012] and Death Valley [Bergmann *et al.*, 2011] also provide evidence that the  $\delta^{13}\text{C}_{\text{carb}}$  excursion was acquired at the time of deposition, a conclusion further supported by subsequent Ca and Mg isotope analyses [Husson *et al.*, 2015]. The mechanism to generate such low  $\delta^{13}\text{C}_{\text{carb}}$  values, however, still remains enigmatic.

Iron isotope ratios provide a useful framework in which to further examine the Shuram excursion. Hydrothermal and weathering inputs are the main sources of Fe delivered to marine sediments and have  $\delta^{56}\text{Fe}$  values near 0‰ [Beard *et al.*, 1999, Chever *et al.*, 2015, Dauphas *et al.*, 2017, Homoky *et al.*, 2013]. Although many processes (e.g., reduction, oxidation, mineral precipitation) fractionate iron isotopes, it is the fractionations commonly observed between Fe(II) and Fe(III) that are thought to be dominant in sedimentary environments [Johnson *et al.*, 2008]. The magnitude of this fractionation is approximately the same whether the transitions are biologically or abiotically mediated, by kinetic or equilibrium processes [Dauphas and Rouxel, 2006]. The bacterial reduction of Fe(III) produces Fe(II) that is depleted in  $\delta^{56}\text{Fe}$  by  $\sim 2\%$  relative to the initial source of Fe [Beard *et al.*, 1999]. Whereas Fe(III) is insoluble at typical pH values for marine waters and sediments, Fe(II) is highly soluble in anoxic waters. This  $^{56}\text{Fe}$ -depleted Fe(II) is mobile and its migration into or out of sediments can result in isotopic shifts to the sedimentary iron pool, driving it away from typical crustal values of  $\sim 0.1\%$ .

Here, we present iron isotope ratio data from Nafun Group strata, Sultanate of Oman to better understand the depositional and diagenetic history of these sediments and the causative mechanism(s) for the Shuram excursion. Because the strata spanning the Shuram excursion are lithologically heterogeneous, we specifically measured the iron associated with the carbonate phase ( $\text{Fe}_{\text{carb}}$ ). Only Fe(II) is partitioned in any abundance into the carbonate mineral lattice [Reeder, 1983] and since ferrous iron is soluble under anoxic conditions, analysis of  $\delta^{56}\text{Fe}_{\text{carb}}$  provides insights into the redox conditions associated with the deposition and subsequent diagenesis of the carbonate fraction.

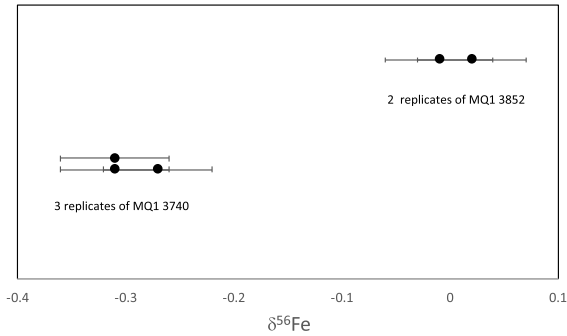


**Figure 1.** Replicated  $\delta^{56}\text{Fe}_{\text{carb}}$  measurements of MQ1 3740 and MQ1 3852.

## 2. Materials and methods

We analyzed subsurface cuttings samples of Nafun Group strata from well MQR-1, which have been previously characterized in detail regarding their sedimentary geology, and carbon and sulfur isotopic composition [Burns and Matter, 1993, Fike *et al.*, 2006]. Cuttings are rock chips (typically 1–5 mm in size) produced during drilling that were collected by the well-site geologist every 2–5 m. Thus, cuttings represent a geochemical and lithologic average, which has the tendency to smooth high-frequency variations sometimes observed in stratigraphic time series data [Fike and Grotzinger, 2008].

Powdered samples of ~150 mg were dissolved in 10 mL of 10% cold acetic acid in an ultrasonic bath for about two hours. The solution was centrifuged and the procedure repeated a second time on the solid residue. Fe was purified by anion-exchange chromatography using the procedure described by Wang *et al.* [2012]. Iron isotopic compositions were measured on a Thermo Scientific Neptune MC-ICP-MS as described by Wang *et al.* [2012]. Reproducibility of the full analytical protocol has been tested by independent analysis of several aliquots from the same powder for multiple samples (e.g., sample MQ1 3740 in triplicate and MQ1 3852 in replicate; Figure 1). For these samples, the  $\delta^{56}\text{Fe}$  of the replicates are in agreement within 0.05‰ ( $2\sigma$ , see Table 1), which is the same order of magnitude as the long-term reproducibility of known standard solutions. On the other hand, replicated measurements of  $\delta^{57}\text{Fe}$  return only a 2SD of 0.30‰. When using these errors all the samples fall on a mass-fractionation line with the expected slope 1.5 in a  $\delta^{57}\text{Fe}$  vs  $\delta^{56}\text{Fe}$

**Table 1.** Fe isotopic data for Nafun Group strata

Sample names	Depth	$\delta^{56}\text{Fe}$	$\delta^{57}\text{Fe}$
MQ1 3240	3240	0.00	0.04
MQ1 3260	3260	0.07	0.16
MQ1 3300	3300	0.11	0.04
MQ1 3320	3320	-0.02	-0.05
MQ1 3350	3350	-0.02	-0.13
MQ1 3360	3360	0.09	0.20
MQ1 3404	3404	0.07	0.19
MQ1 3428	3428	0.00	-0.16
MQ1 3510	3510	-0.11	0.02
MQ1 3530	3530	-0.37	-0.67
MQ1 3556	3556	-0.55	-0.71
MQ1 3600	3600	-1.05	-1.55
MQ1 3620	3620	-0.77	-1.22
MQ1 3636	3636	-0.94	-1.35
MQ1 3660	3660	-0.57	-1.00
MQ1 3700	3700	-0.38	-0.41
MQ1 3722	3722	-0.29	-0.48
MQ1 3740 <sup>a</sup>	3740	-0.27	-0.62
MQ1 3740 <sup>b</sup>	3740	-0.31	-0.36
MQ1 3740 <sup>c</sup>	3740	-0.31	-0.57
MQ1 3756	3756	-0.29	-0.16
MQ1 3780	3780	-0.15	-0.09
MQ1 3800	3800	-0.11	-0.12
MQ1 3806	3806	-0.26	-0.27
MQ1 3810	3810	-0.44	-0.66
MQ1 3826	3826	0.10	0.16
MQ1 3832	3832	0.05	-0.08
MQ1 3848	3848	0.04	0.02
MQ1 3852 <sup>a</sup>	3852	0.02	-0.16
MQ1 3852 <sup>b</sup>	3852	-0.01	0.06
MQ1 3860	3860	0.00	-0.03
MQ1 3880	3880	-0.09	-0.23
MQ1 3900	3900	0.06	0.00
MQ1 3920	3920	0.11	0.16
MQ1 3926	3926	0.04	0.11
MQ1 3932	3932	0.05	0.12
MQ1 3936	3936	0.06	0.00
MQ1 3948	3948	-0.15	-0.40

(continued on next page)

**Table 1.** (continued)

Sample names	Depth	$\delta^{56}\text{Fe}$	$\delta^{57}\text{Fe}$
MQ1 3970	3970	0.08	0.04
MQ1 3984	3984	0.10	0.12
MQ1 4000	4000	-0.03	-0.11

Fe isotopic compositions ( $\delta^{56}\text{Fe}$ ) of the carbonate fraction, reported in permil ( $\text{‰}$ ) relative to the terrestrial standard IRMM014. Note: a, b and/or c indicate laboratory replicates (dissolution, chemical purification, and mass-spectrometry analysis) of a given sample. The precision of these independent replicates is in the same range as the reproducibility of the standard ( $2\sigma = 0.05\text{‰}$  for  $\delta^{56}\text{Fe}$ ) and is much smaller than the range of isotopic fractionation ( $1\text{‰}$ ) observed in this study.

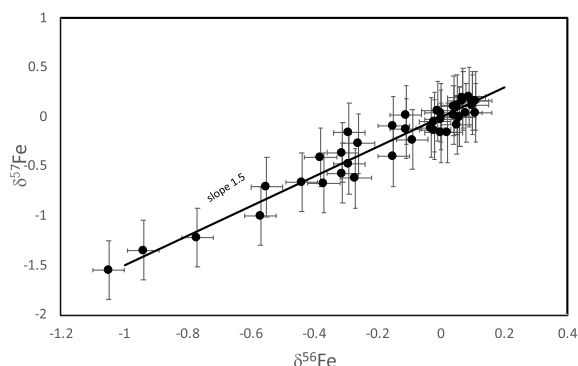


**Figure 2.** Triple isotope diagram ( $\delta^{57}\text{Fe}$  vs  $\delta^{56}\text{Fe}$ ) for all the samples analyzed here. All the samples fall on a mass-fractionation line of slope 1.5.

plot (Figure 2). Given the mass-dependency relationship and the better reproducibility of the  $\delta^{56}\text{Fe}$ , we will discuss all the data in terms of  $\delta^{56}\text{Fe}$ .

### 3. Results

Nafun Group sediments analyzed in the present study were deposited from 635–548 Ma in a regionally extensive sag basin under open, shallow marine conditions, and each formation can be traced laterally for several hundred km across Oman

[Bowring *et al.*, 2007, Grotzinger *et al.*, 2002, Le Guerroue *et al.*, 2006a, Mattes and Conway-Morris, 1990, McCarron, 2000]. The strata comprise two clastic-to-carbonate shallowing-upward successions (Masirah Bay Formation (Fm.) and Khufai Fm.; Shuram Fm. and Buah Fm.). The Shuram excursion spans several hundred meters of section from the uppermost Khufai Fm. through Shuram Fm. and into the mid-Buah Fm. [Burns and Matter, 1993, Fike *et al.*, 2006, Le Guerroue *et al.*, 2006b]. The Shuram excursion has been identified in multiple sections, both from outcrops and the subsurface, and serves as an excellent stratigraphic marker for correlation across Oman [Burns and Matter, 1993, Le Guerroue *et al.*, 2006a, McCarron, 2000].

Nafun Group strata have  $\delta^{56}\text{Fe}_{\text{carb}}$  values that range between  $-1.05\text{‰}$  to  $+0.24\text{‰}$  and preserve a record of stratigraphically coherent variations with small scatter between successive sample data points (Figure 3). Masirah Bay and Khufai strata possess  $\delta^{56}\text{Fe}_{\text{carb}}$  isotopic compositions typical of bulk crustal materials ( $\sim 0.1\text{‰}$ ). However, a progressive drop in  $\delta^{56}\text{Fe}_{\text{carb}}$  values, down to  $-1.05\text{‰}$  characterizes the stratigraphic interval of the Shuram excursion. This  $\delta^{56}\text{Fe}_{\text{carb}}$  minimum is stratigraphically offset from the nadir of the  $\delta^{13}\text{C}_{\text{carb}}$  excursion. As the  $\delta^{13}\text{C}_{\text{carb}}$  excursion ends, there is a gradual return to “typical” terrestrial  $\delta^{56}\text{Fe}_{\text{carb}}$  values ( $\sim 0.1\text{–}0.2\text{‰}$ ), which are retained in the overlying Buah strata.

Complementary data from iron speciation and TOC abundance are also presented. Iron speciation data (Figure 3) show high ratios of pyrite to total iron in the Masirah Bay and Khufai formations. At the onset of the Shuram excursion, there is a substantial drop in pyrite to total iron ratios, in parallel with a large increase in total iron. This increase is coincident with increased siliciclastic input (based on parallel increases in Ti abundance). In the upper Buah Fm., following the recovery of the Shuram excursion, there is a slight increase in pyrite to total iron ratios and a return to baseline total iron concentrations, corresponding to a decrease in siliciclastic input (Figure 3). TOC contents vary strongly in upsection (Figure 3): Masirah Bay and Khufai Nafun strata are characterized by relatively high TOC ( $>1\text{‰}$ ), whereas the Shuram and lowermost Buah strata coincident with low  $\delta^{56}\text{Fe}$  values have minimal TOC ( $<0.1\text{‰}$ ), and TOC levels increase slightly in the upper Buah (although remaining below 1%).

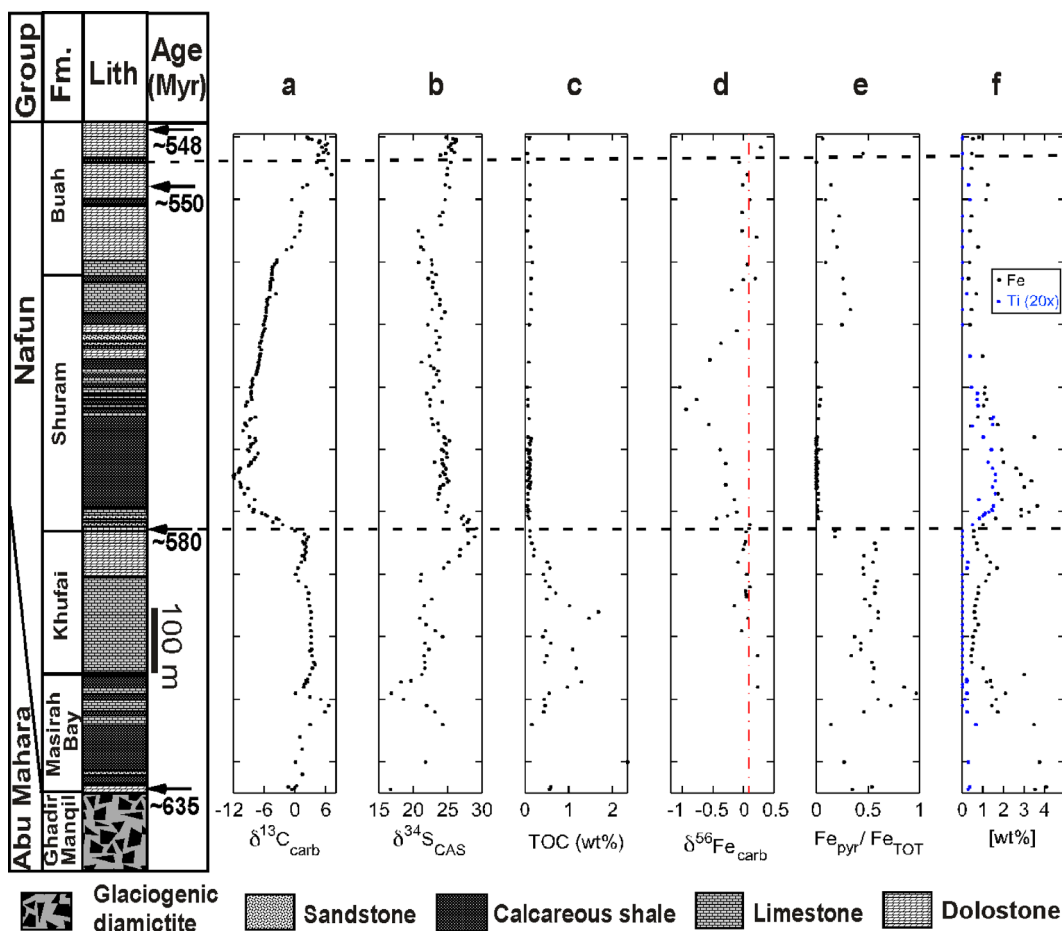


**Figure 3.** Isotopic and geochemical data from well MQR-1 through the Nafun Group strata, plotted alongside a stratigraphic column. Data shown are  $\delta^{13}\text{C}_{\text{carb}}$ ,  $\delta^{34}\text{S}_{\text{CAS}}$  (carbonate-associated sulfate), TOC (wt%),  $\delta^{56}\text{Fe}_{\text{carb}}$ ,  $\text{Fe}_{\text{pyr}}/\text{Fe}_{\text{TOT}}$  (iron in pyrite relative to total iron), and total iron and titanium (at  $20\times$  abundance), both in wt%. The red dashed lines indicate bulk terrestrial  $\delta^{56}\text{Fe}$  (0.1‰). Age dates come from correlation based on  $\delta^{13}\text{C}_{\text{carb}}$  chemostratigraphy [Bowring *et al.*, 2007, Fike *et al.*, 2006]. Carbon and sulfur isotope and TOC data are from Fike *et al.* [2006].

#### 4. Discussion

The  $\delta^{56}\text{Fe}_{\text{carb}}$  data provide new constraints on redox conditions prior to, during, and in the aftermath of the Shuram excursion. Without knowing the isotopic composition and relative abundance of all iron-bearing phases at the time of deposition, it is not possible to rigorously interpret a given  $\delta^{56}\text{Fe}_{\text{carb}}$  value for a unique set of processes. We can, however, draw several end-member expectations for iron isotope ratios as a function of the redox state and processes in the sedimentary environment.

Strata in the Masirah Bay and Khufai have  $\delta^{56}\text{Fe}_{\text{carb}}$  values of  $\sim 0.1\text{‰}$  and are characterized by high TOC, abundant pyrite, and enrichments in redox-sensitive trace elements. In organic-rich sediments, such as these, all reactive ferric iron is reduced to Fe(II) and thus liable to be incorporated into  $\text{Fe}_{\text{carb}}$ . For reasons of isotope mass balance, the reduction of the readily biologically available iron oxides (hereafter referred to as quantitative iron reduction) results in a  $\delta^{56}\text{Fe}_{\text{carb}}$  signature of  $\sim 0.1\text{‰}$  for a sample with composition similar to typical crustal materials. Depositional conditions for these strata

were previously inferred to be anoxic to euxinic [Fike and Grotzinger, 2008, Fike et al., 2006, Wu et al., 2015] and the  $\delta^{56}\text{Fe}_{\text{carb}}$  values presented here are consistent with complete reduction of available iron oxides.

Strata in the upper Buah Fm. are also characterized by  $\delta^{56}\text{Fe}_{\text{carb}}$  values of  $\sim 0.1\%$ . However, iron speciation,  $\Delta^{33}\text{S}$  data, and the distribution of redox-sensitive trace elements suggest that depositional conditions in these strata were oxic [Fike and Grotzinger, 2008, Fike et al., 2006, Wu et al., 2015]. Both TOC and pyrite are found in very low levels in these strata. While organic carbon is not overly abundant ( $<1\%$ ), it was sufficient to reduce the much smaller reservoir of iron oxides. Consistent with these observations, the  $\delta^{56}\text{Fe}_{\text{carb}}$  again approximates bulk silicate values ( $\sim 0.1\%$ ), supporting complete reduction of available iron oxides.

In contrast, the strata containing the Shuram  $\delta^{13}\text{C}_{\text{carb}}$  excursion are characterized by exceptionally low  $\delta^{56}\text{Fe}_{\text{carb}}$  values (down to  $-1.05\%$ ). These strata are also characterized by very low ( $<0.1\%$ ) residual TOC and low pyrite abundances; nearly complete consumption of available organics may explain the relatively enriched  $\delta^{13}\text{C}_{\text{org}}$  values from this core and their high stratigraphic scatter [Fike et al., 2006], making them unreliable indicators of ambient carbon cycling [Dehler et al., 2005, Johnston et al., 2012]. In addition, both iron speciation and the distribution of redox-sensitive trace elements point to oxidizing conditions during deposition.

During deposition of these strata, TOC abundance was sufficient to reduce just a fraction of the available ferric iron. As such, the isotopic signature of the resulting ferrous iron is expected to express a large part of the fractionation ( $\sim 2\%$ ) associated with iron reduction [Beard et al., 1999]. Specifically, carbonates forming in these environments of incomplete iron reduction would be expected to have lower  $\delta^{56}\text{Fe}_{\text{carb}}$  values relative to available ferric iron, which is the signal observed during the Shuram excursion (Figure 3). The low  $\delta^{56}\text{Fe}$  values in these strata preclude reduction of the majority of the available pool of ferric oxides. This partial reduction of ferric oxides resulted in the generation of a local  $^{56}\text{Fe}$ -depleted Fe(II) reservoir incorporated into the carbonates precipitating at the sediment–water interface and the underlying sediments (i.e., during deposition and early diagenesis).

While the migration of Fe(II) is limited in strictly oxic or euxinic environments by rapid and nearly quantitative conversion to iron oxyhydroxides or iron sulfides, respectively, the mobilization and net migration of  $^{56}\text{Fe}$ -depleted Fe(II) can occur under ferruginous (anoxic but not sulfidic) conditions. For example, net migration of dissolved iron occurs in the modern Black Sea, where Fe(II) diffuses out of sediments beneath anoxic waters following *in situ* reduction and can subsequently be transported along the chemocline [Anderson and Raiswell, 2004, Wijsman et al., 2001]. As such, the presence of a ferruginous iron source during Shuram time could explain the low  $\delta^{56}\text{Fe}_{\text{carb}}$  values observed [Severmann et al., 2006]. However, the smooth stratigraphic profile observed in our  $\delta^{56}\text{Fe}_{\text{carb}}$  data would also require a gradual onset and cessation for the advection of ferruginous waters, a situation that we view as unlikely given the high-energy depositional environment of these strata (e.g., as evidenced by hummocky cross-stratified intraclast–oid grainstones) [Bergmann, 2013, Grotzinger et al., 2011, Le Guerroue et al., 2006a]. Moreover, the minimum in  $\delta^{56}\text{Fe}_{\text{carb}}$  is observed to coincide with the minimum in TOC abundance, stratigraphically above the nadir in  $\delta^{13}\text{C}_{\text{carb}}$  (Figure 3), a correlation not readily explained by a marine ferruginous iron source.

Thus, the stratigraphic expression of the  $\delta^{56}\text{Fe}$  signal observed during the Shuram excursion is more likely to reflect local redox conditions within the sediments during and following deposition. This is inferred to be mediated primarily by the abundance of organic carbon relative to that of oxidized iron-bearing phases delivered to the sediments [Bergmann, 2013]. Specifically, the  $\delta^{56}\text{Fe}$  data show that there was never more organic matter present than reactive iron during the formation of the carbonates recording the Shuram excursion (be it in the water column, during sedimentary lithification, or during late diagenesis). This observation effectively excludes late-stage burial diagenesis [Derry, 2010b] as a potential source of the Shuram excursion. The  $\text{Fe}_{\text{carb}}$  isotopic composition during the Shuram excursion thus was controlled by the relative abundance of organic C and oxidized Fe delivery to sediments [Bergmann, 2013, Bergmann et al., 2013], while the carbon isotopic signature is controlled by the residence time of carbon in the ocean/atmosphere. A decoupling between these two

timescales could produce the observed stratigraphic decoupling in the isotopic composition of these systems.

The strata recording the Shuram excursion are associated with increased detrital contribution of wind-blown silt [Bergmann, 2013], likely replete with iron oxides (as is seen Saharan dust today). Interestingly, increased detrital input and enhanced iron delivery are also seen associated with the Shuram excursion in the coeval Johnnie Fm. (Death Valley, CA) [Bergmann *et al.*, 2013]. Together, these suggest that both enhanced oxidative weathering on the continents and the subsequent delivery of detrital iron oxides to marine sediments played a role in the origin and timing of the Shuram excursion. This enhanced flux of iron oxides led to an oxidative pulse in marine sediments and a partial reduction of these oxides is the most parsimonious explanation of the stratigraphically coherent variations observed in  $\delta^{56}\text{Fe}_{\text{carb}}$  during the Shuram excursion. The associated oxidation of organic matter can help explain both the characteristic depletion in  $\delta^{13}\text{C}_{\text{carb}}$  that constitutes the Shuram excursion as well as the abnormally low net organic carbon burial observed globally during this interval [Bergmann *et al.*, 2011, Calver, 2000, Fike and Grotzinger, 2007, Kaufman *et al.*, 2007, McFadden *et al.*, 2008].

These data add to the growing body of work that suggests the Shuram  $\delta^{13}\text{C}_{\text{carb}}$  excursion was formed at the time of deposition, either reflecting a primary perturbation to the marine carbon cycle, or, if diagenetic in origin, mediated by a novel, global means to “precondition” sediments for subsequent chemical modification during deposition or shortly thereafter [e.g., Grotzinger *et al.*, 2011]. Our results suggest further that this preconditioning could be mediated by enhanced transport of terrestrial iron oxides to the sediments. Through microbial iron reduction (and associated abiotic reactions), these iron oxide phases would have consumed existing reducing pools within the sediments and overlying water column (including e.g., hypothesized reservoirs of dissolved organic carbon; [Rothman *et al.*, 2003]). The associated oxidation of organic carbon during Shuram time gave rise to C isotope patterns that were essentially global in scope and timing. As such, be it a primary signature of the water column or a unique example of “global sedimentary diagenesis”, these data point to the mid-Ediacaran as a time of increasingly oxidized

conditions that set the stage for the appearance and subsequent evolutionary radiation of metazoa.

The redox composition of recently deposited sediments serves as an important buffer on atmospheric oxygen concentrations. The oxygen demand by chemical weathering is directly related to the abundance of electron-rich substrates (e.g., organic matter, pyrite, ferrous silicates, and carbonates) in sedimentary rocks. All else being equal, a more reducing reservoir translates to more oxygen demand and lower atmospheric oxygen concentrations [Bernier, 2006]. We suggest that the Shuram excursion represents the terminal loss of a long-lived reducing reservoir, one titrated out by enhanced delivery of detrital iron oxides. The oxidation of these surficial sediments would consume a much smaller oxidant pool than that needed to ventilate an anoxic deep ocean [e.g., Fike *et al.*, 2006], in line with modeled constraints on oxidant budgets [Bristow and Kennedy, 2008, Le Guerroue *et al.*, 2006b]. Furthermore, this transition spanning the Shuram excursion was accomplished over a protracted interval [Bowring *et al.*, 2007, Rooney *et al.*, 2020] characterized by very low net organic carbon burial in marine sediments.

In a strict budgetary sense, these processes represent a transient drop in oxygen levels on the fluid Earth associated with the oxidation of these reduced sediments (i.e., generating the Shuram  $\delta^{13}\text{C}$  excursion). However, once this buffer was removed, reorganization of the major sinks on oxygen may have subsequently allowed  $\text{pO}_2$  levels to rise to higher levels (e.g., 10% or greater) typical of the Phanerozoic. Our observations are consistent with previous reports of a transition in the redox composition of the sediments toward more oxidizing conditions displayed in other Ediacaran-age strata (e.g., Canfield *et al.*, 2007), but see Sperling *et al.* [2015]), and directly connect the Shuram excursion to this transition. By removing a long-lived reducing sedimentary buffer, this event set the stage for atmospheric oxygen to rise, promoting the diversification of the metazoa.

## Acknowledgments

FM thanks the Academie des Sciences et l’Institut de France for the Prix Mme Victor Noury and to have the possibility to submit this paper. We deeply appreciate

constructive comments from two anonymous reviewers and from the editor Francois Chabaux, which greatly improved this manuscript. FM acknowledges funding from the European Research Council under the H2020 framework program/ERC grant agreement (#637503-PRISTINE) and financial support of the UnivEarthS Labex program at Sorbonne Paris Cité (#ANR-10-LABX-0023 and #ANR-11-IDEX-0005-02), and the ANR through a chaire d'excellence Sorbonne Paris Cité. Parts of this work were supported by IGP multidisciplinary program PARI, and by Region île-de-France SESAME Grant (no. 12015908). We thank the Oman Ministry of Oil and Gas for permission to publish this paper. This research was supported by Petroleum Development Oman (PDO) and a grant from the Agouron Institute to D.A.F. and W.W.F. We would like to thank PDO for access to samples and logistical support.

## References

- Anderson, T. F. and Raiswell, R. (2004). Sources and mechanisms for the enrichment of highly reactive iron in euxinic Black Sea sediments. *Am. J. Sci.*, 304, 203–233.
- Beard, B. L., Johnson, C. M., Cox, L., Sun, H., Neaslon, K. H., and Aguilar, C. (1999). Iron isotope biosignature. *Science*, 285, 1889–1892.
- Bergmann, K. D. (2013). *Constraints on the carbon cycle and climate during the early evolution of animals*. PhD thesis, California Institute of Technology, Pasadena. 417 pages.
- Bergmann, K. D., Grotzinger, J. P., and Fischer, W. W. (2013). Biological influences on seafloor carbonate precipitation. *Palaios*, 28, 99–115.
- Bergmann, K. D., Zentmyer, R. A., and Fischer, W. W. (2011). The stratigraphic expression of a large negative carbon isotope excursion from the Ediacaran Johnnie Formation. *Death Valley Precambrian Res.*, 188, 45–56.
- Berner, R. (2006). GEOCARBSULF: A combined model for Phanerozoic atmospheric O<sub>2</sub> and CO<sub>2</sub>. *Geochim. Cosmochim. Acta*, 70, 5653–5664.
- Bowring, S. A., Grotzinger, J. P., Condon, D. J., and Ramezani, J. (2007). Geochronologic constraints on the chronostratigraphic framework of the Neoproterozoic Huqf Supergroup, Sultanate of Oman. *Am. J. Sci.*, 307, 1097–1145.
- Bristow, T. F. and Kennedy, M. J. (2008). Carbon isotope excursions and the oxidant budget of the Ediacaran atmosphere and ocean. *Geology*, 36, 863–866.
- Burns, S. J. and Matter, A. (1993). Carbon isotopic record of the latest Proterozoic from Oman. *Eclogae Geologicae Helveticae*, 86, 595–607.
- Calver, C. R. (2000). Isotope stratigraphy of the Ediacaran (Neoproterozoic III) of the Adelaide Rift Complex, Australia, and the overprint of water-column stratification. *Precamb. Res.*, 100, 121–150.
- Canfield, D. E., Poulton, S. W., and Narbonne, G. M. (2007). Late-Neoproterozoic deep-ocean oxygenation and the rise of animal life. *Science*, 315, 92–95.
- Chever, F., Rouxel, O., Croot, P., Ponzevera, E., Wuttig, K., and Auro, M. (2015). Total dissolvable and dissolved iron isotopes in the water column of the Peru upwelling regime. *Geochim. Cosmochim. Acta*, 162, 66–82.
- Dauphas, N., John, S. G., and Rouxel, O. (2017). Iron isotope systematics. In Teng, F.-Z., Watkins, J., and Dauphas, N., editors, *Non-traditional Stable Isotopes*, pages 415–510. Mineralogical Society of America, Chantilly, Virginia.
- Dauphas, N. and Rouxel, O. (2006). Mass spectrometry and natural variations of iron isotopes. *Mass Spectrom. Rev.*, 25, 515–550.
- Dehler, C. M., Elrick, M., Bloch, J. D., Crossey, L. J., Karlstrom, K. E., and Des Marais, D. J. (2005). High-resolution delta C-13 stratigraphy of the Chuar Group (ca. 770–742 Ma), Grand Canyon: Implications for mid-Neoproterozoic climate change. *Geol. Soc. Am. Bull.*, 117, 32–45.
- Derry, L. (2010a). A burial diagenesis origin for the Ediacaran Shuram-Wonoka carbon isotope anomaly. *Earth Planet. Sci. Lett.*, 194, 151–162.
- Derry, L. (2010b). On the significance of  $\delta^{13}\text{C}$  correlations in ancient sediments. *Earth Planet. Sci. Lett.*, 296, 497–501.
- Fike, D. and Grotzinger, J. (2007). The evolution of the ediacaran sulfur cycle: A paired sulfate-pyrite delta S-34 approach. *Geochim. Cosmochim. Acta*, 71, A278–A278.
- Fike, D. A. and Grotzinger, J. P. (2008). A paired sulfate-pyrite  $\delta^{34}\text{S}$  approach to understanding the evolution of the Ediacaran-Cambrian sulfur cycle. *Geochim. Cosmochim. Acta*, 72, 2636–2648.
- Fike, D. A., Grotzinger, J. P., Pratt, L. M., and Summons, R. E. (2006). Oxidation of the Ediacaran

- Ocean. *Nature*, 444, 744–747.
- Grotzinger, J. P., Al-Siyabi, A. H., Al-Hashimi, R. A., and Cozzi, A. (2002). New model for tectonic evolution of Neoproterozoic-Cambrian Huqf Super-group basins. *Oman. GeoArabia*, 7, 241.
- Grotzinger, J. P., Fike, D. A., and Fischer, W. W. (2011). Enigmatic origin of the largest known carbon isotope excursion in Earth's history. *Nat. Geosci.*, 4, 285–292.
- Homoky, W. B., John, S. G., Conway, T., and Mills, R. A. (2013). Distinct iron isotopic signatures and supply from marine sediment dissolution. *Nat. Commun.*, 4, article no. 2143.
- Husson, J. M., Higgins, J. A., Maloof, A. C., and Schoene, B. (2015). Ca and Mg isotope constraints on the origin of Earth's deepest  $\delta^{13}\text{C}$  excursion. *Geochim. Cosmochim. Acta*, 160, 243–266.
- Husson, J. M., Maloof, A. C., and Schoene, B. (2012). A syn-depositional age for Earth's deepest  $\delta^{13}\text{C}$  excursion required by isotope conglomerate tests. *Terra Nova*, 24, 318–325.
- Johnson, C. M., Beard, B. L., and Roden, E. E. (2008). The iron isotope fingerprints of redox and biogeochemical cycling in modern and ancient Earth. *Annu. Rev. Earth Planetary Sci.*, 36, 457–493.
- Johnston, D. T., Macdonald, F. A., Gill, B. C., Hoffman, P. F., and Schrag, D. P. (2012). Uncovering the Neoproterozoic carbon cycle. *Nature*, 483, article no. 320-U110.
- Kaufman, A. J., Corsetti, F. A., and Varni, M. A. (2007). The effect of rising atmospheric oxygen on carbon and sulfur isotope anomalies in the Neoproterozoic Johnnie Formation, Death Valley, USA. *Chem. Geol.*, 237, 47–63.
- Knauth, L. P. and Kennedy, M. J. (2009). The late Precambrian greening of the Earth. *Nature*, 460, 728–732.
- Le Guerroue, E., Allen, P. A., and Cozzi, A. (2006a). Chemostratigraphic and sedimentological framework of the largest negative carbon isotopic excursion in Earth history: The Neoproterozoic Shuram Formation (Nafun Group, Oman). *Precambrian Res.*, 146, 68–92.
- Le Guerroue, E., Allen, P. A., and Cozzi, A. (2006b). Parasequence development in the Ediacaran Shuram Formation (Nafun Group, Oman): high-resolution stratigraphic test for primary origin of negative carbon isotopic ratios. *Basin Res.*, 18, 205–219.
- Lee, C., Fike, D. A., Love, G. D., Sessions, A. L., Grotzinger, J. P., Summons, R. E., and Fischer, W. W. (2013). Carbon isotopes and lipid biomarkers from organic-rich facies of the Shuram Formation, Sultanate of Oman. *Geobiology*, 11, 406–419.
- Lee, C., Love, G. D., Fischer, W. W., Grotzinger, J. P., and Halverson, G. P. (2015). Marine organic matter cycling during the Ediacaran Shuram excursion. *Geology*, 43, 1103–1106.
- Mattes, B. W. and Conway-Morris, S. (1990). Carbonate/evaporite deposition in the Late Precambrian–Early Cambrian Ara Formation of southern Oman. In Robertson, A. H. F., Searle, M. P., and Ries, A. C., editors, *The Geology and Tectonics of the Oman Region*. Geological Society, London.
- McCarron, G. (2000). *The Sedimentology and Chemostratigraphy of the Nafun Group, Huqf Supergroup*. Oxford University, Oman.
- McFadden, K. A., Huang, J., Chu, X., Jiang, G., Kaufman, A. J., Zhou, C., Yuan, X., and Xiao, S. (2008). Pulsed oxidation and biological evolution in the Ediacaran Doushantuo Formation. *Proc. Natl Acad. Sci. USA*, 105, 3197–3202.
- Reeder, R. J. (1983). Crystal chemistry of the rhombohedral carbonates. In *Reviews in Mineralogy and Geochemistry*, pages 1–47. Mineralogical Society of America, Chantilly, Virginia.
- Rooney, A., Cantine, M., Bergmann, K., Gomez-Perez, I., Al Baloushi, B., Boag, T., Busch, J., Sperling, E., and Strauss, J. (2020). *Proc. Natl Acad. Sci. USA*, 117, 16824–16830.
- Rothman, D. H., Hayes, J. M., and Summons, R. E. (2003). Dynamics of the Neoproterozoic carbon cycle. *Proc. Natl Acad. Sci. USA*, 100, 8124–8129.
- Severmann, S., Johnson, C. M., Beard, B. L., and McManus, J. (2006). The effect of early diagenesis on the Fe isotope compositions of porewaters and authigenic minerals in continental margin sediments. *Geochim. Cosmochim. Acta*, 70, 2006–2022.
- Sperling, E. A., Wolock, C. J., Morgan, A. S., Gill, B. C., Kunzmann, M., Halverson, G. P., Macdonald, F. A., Knoll, A. H., and Johnston, D. T. (2015). Statistical analysis of iron geochemical data suggests limited late Proterozoic oxygenation. *Nature*, 523, 451–454.
- Swart, P. K. (2008). Global synchronous changes in the carbon isotopic composition of carbonate sediments unrelated to changes in the global carbon cycle. *Proc. Natl Acad. Sci. USA*, 105, 13741–13745.
- Wang, K., Moynier, F., Dauphas, N., Barrat, J. A., Crad-

- dock, P., and Sio, C. K. (2012). Iron isotope fractionation in planetary crusts. *Geochim. Cosmochim. Acta*, 89, 31–45.
- Wijsman, J. W. M., Middelburg, J. J., and Heip, C. H. R. (2001). Reactive iron in Black Sea Sediments: implications for iron cycling. *Marine Geol.*, 172, 167–180.
- Wu, N., Farquhar, J., and Fike, D. A. (2015). Ediacaran sulfur cycle: Insights from sulfur isotope measurements ( $\delta^{34}\text{S}$  and  $\Delta^{33}\text{S}$ ) on paired sulfate-pyrite in the Huqf Supergroup of Oman. *Geochim. Cosmochim. Acta*, 164, 352–364.